Research

Multi-tissue gene-expression analysis in a mouse model of thyroid hormone resistance

Lance D Miller[*], Peter McPhie[†], Hideyo Suzuki[‡], Yasuhito Kato[‡], Edison T Liu[*] and Sheue-yann Cheng[‡]

Addresses: [*]Genome Institute of Singapore, Agency for Science, Technology and Research, 60 Biopolis Street, Singapore, 138672. [†]National Institute of Diabetes and Digestive and Kidney Diseases, National Institutes of Health, Bethesda, MD 20892, USA. [‡]Laboratory of Molecular Biology, National Cancer Institute, Bethesda, MD 20892-4264, USA.

Correspondence: Sheue-yann Cheng. E-mail: sycheng@helix.nih.gov

Published: 29 April 2004

Genome ***Biology*** 2004, **5:**R31

The electronic version of this article is the complete one and can be found online at http://genomebiology.com/2004/5/5/R31

Received: 19 February 2004
Revised: 16 March 2004
Accepted: 1 April 2004

Abstract

Background: Resistance to thyroid hormone (RTH) is caused by mutations of the thyroid hormone receptor β (TRβ) gene. To understand the transcriptional program underlying TRβ mutant-induced phenotypic expression of RTH, cDNA microarrays were used to profile the expression of 11,500 genes in a mouse model of human RTH.

Results: We analyzed transcript levels in cerebellum, heart and white adipose tissue from a knock-in mouse ($TR\beta^{PV/PV}$ mouse) that harbors a human mutation (referred to as PV) and faithfully reproduces human RTH. Because $TR\beta^{PV/PV}$ mice have elevated thyroid hormone (T3), to define T3-responsive genes in the context of normal TRβ, we also analyzed T3 effects in hyperthyroid wild-type gender-matched littermates. Microarray analysis revealed 163 genes responsive to T3 treatment and 187 genes differentially expressed between $TR\beta^{PV/PV}$ mice and wild-type littermates. Both the magnitude and gene make-up of the transcriptional response varied widely across tissues and conditions. We identified genes modulated in T3-dependent PV-independent, T3- and PV-dependent, and T3-independent PV-dependent pathways that illuminated the biological consequences of PV action *in vivo*. Most T3-responsive genes that were dysregulated in the heart and white adipose tissue of $TR\beta^{PV/PV}$ mice were repressed in T3-treated wild-type mice and upregulated in $TR\beta^{PV/PV}$ mice, suggesting the inappropriate activation of T3-suppressed genes in RTH.

Conclusions: Comprehensive multi-tissue gene-expression analysis uncovered complex multiple signaling pathways that mediate the molecular actions of TRβ mutants *in vivo*. In particular, the T3-independent mutant-dependent genomic response unveiled the contribution of a novel 'change-of-function' of TRβ mutants to the pathogenesis of RTH. Thus, the molecular actions of TRβ mutants are more complex than previously envisioned.

Background

Thyroid hormone (T3) regulates growth, development and differentiation. These actions are mediated by high-affinity thyroid hormone receptors (TRs) that bind T3 and localize to the nucleus, where they regulate transcription of target genes. Four T3-binding TR isoforms, β1, β2, β3 and α1, are derived from two TR genes (β and α genes) by alternative splicing of the primary transcripts [1-3]. The expression of these TR isoforms is tissue dependent and developmentally regulated [1,2,4]. As transcription factors, the TRs regulate gene expression by binding thyroid-hormone response elements (TREs) in the regulatory domains of target genes which can confer specificity for TR isoforms [5]. The transcriptional activity of the TRs is also modulated by a host of co-repressors and co-activators [6].

Mutations in TRβ that affect its ability to bind T3 or interact with co-repressors results in the syndrome known as resistance to thyroid hormone (RTH) [7-9]. RTH is a dominantly inherited abnormality that manifests as an impaired sensitivity of thyroid hormone-responsive tissues to circulating T3 [7,9]. Clinical diagnosis of RTH typically recognizes elevated levels of thyroid hormone associated with nonsuppressible thyroid-stimulating hormone (TSH) [7,9]. The clinical presentation of the disease is hypothyroidism, with symptoms such as delayed growth, cognitive dysfunction, and hypercholesterolemia, and, concurrently, signs consistent with hyperthyroidism, including tachycardia, weight loss, attention deficit-hyperactivity disorder and advanced bone age. The hypothyroid-like effects are presumably the consequence of mutant TRβ interference with, or inhibition of, normal T3 signaling pathways, whereas the signs reflective of hyperthyroidism result from the elevated T3 driving the activity of the TRα1 isoform [10].

To investigate the physiological consequences of a mutant β receptor in the germline, a mouse model expressing a TRβ mutant was created using homologous recombination and the Cre/loxP system [11]. The targeted TRβ mutation (referred to as PV) was the same as that from a patient with severe RTH whose symptoms included elevated T3 and T4, nonsuppressible TSH, goiter, tachycardia and short stature [12]. The PV mutant was shown *in vitro* to lack both T3-binding activity and transcriptional capacity and to strongly interfere with the transcriptional activity of normal TRs [12]. The PV mutant was found expressed in all mouse T3-target tissues examined, including cerebrum, cerebellum, pituitary, liver, brown and white adipocytes, heart, muscle, lung, spleen and kidney [11]. TRβPV mice exhibited goiter, delayed bone development, impaired weight gain, hearing defects and hypercholesterolemia, all of which are reminiscent of the clinical presentation of RTH in humans [11,13,14].

The availability of this mouse model provides an extraordinary opportunity to understand the molecular actions of TRβ mutants and to elucidate the affected cellular pathways *in vivo*. To this end, we applied high-density cDNA microarrays to identify PV-affected genes in the heart, cerebellum and white adipose tissue (WAT) of $TR\beta^{PV/PV}$ mice. Concurrently, we analyzed the expression profiles of wild-type littermates treated with T3 to uncover T3-responsive genes in the context of normal TRβ in a model of pharmacologic hyperthyroidism. Across the three tissues analyzed, we identified (by twofold change or more) 163 distinct genes responsive to T3 treatment and 187 genes differentially expressed between $TR\beta^{PV/PV}$ mice and wild-type littermates.

The expression patterns of these genes showed a diverse transcriptional response comprising genes with tissue-specific expression and genes with similar or contrasting expression in multiple tissues. Category analysis of expression patterns identified genes that were modulated by T3-dependent PV-independent, T3- and PV-dependent, and T3-independent PV-dependent mechanisms. Intra-tissue expression analysis provided a biological glimpse of the adverse effects of PV in a tissue-dependent manner. Finally, hierarchical clustering of multi-tissue gene-expression patterns revealed evidence of discrete biological pathways including immune response, lipogenesis and cell-cycle inhibition that are modulated in multiple tissues of hyperthyroid and T3-resistant $TR\beta^{PV/PV}$ mice. These findings provide a molecular framework for understanding the variability in tissue sensitivity of RTH and provide insight into signaling pathways of mutant TRβ *in vivo*.

Results

Experimental design

RTH, caused by mutation of the TRβ gene, is the consequence of abnormal transcription of thyroid-hormone-responsive genes in T3 target tissues. Using a mouse cDNA microarray containing 11,500 gene probes (representing over 10,000 unique named and unnamed expressed sequence tags (ESTs)), we profiled gene-expression patterns in mouse models of hyperthyroidism and RTH to reveal T3-responsive (hyperthyroid-associated) and mutant PV-dysregulated genes. The three T3-target tissues profiled in this study were the cerebellum, heart and WAT, all of which are important T3-target tissues in which T3-responsive genes have yet to be comprehensively analyzed. The experimental comparisons in this study included: wild-type mice versus $TR\beta^{PV/PV}$ littermates (the RTH group); wild-type mice injected with T3 versus those receiving saline injection only (the iT3 group); and wild-type mice versus a second set of wild-type animals selected in the same way (the control group).

In the RTH experiments, we identified changes in gene expression resulting from the *in vivo* action of PV and/or elevated T3 characteristic of clinical RTH. The iT3 experiments revealed genes that are responsive to increased levels of T3 in pharmacologic hyperthyroidism. These experiments allowed us to analyze the expression profiles in RTH that are the

effects due to the increased levels of circulating thyroid hormone and thus to understand which TR-subtype-dependent transcriptional mechanisms govern gene expression. The purpose of the control group was to identify genes that naturally fluctuate as the result of normal inter-animal differences [15]. Genes identified as differentially expressed in the control group were subsequently censored in a tissue-dependent manner. For each experimental comparison, replicate microarray hybridizations were performed with reciprocal labeling (dye-swapping) to minimize technical noise (see Materials and methods).

Identification and characterization of T3-responsive genes

Differentially expressed genes (outliers) were selected based on the 2.0*r* criterion whereby the fold change detected on each of two reciprocally labeled arrays (*r* designation) was greater than twofold (up or down, but in a reciprocal manner) in at least one experimental comparison. The average expression ratios were calculated as described (see Materials and methods) and are used herein as the expression ratio measurements. To evaluate the probe-level reproducibility of the microarray data, we examined the variability of the expression ratios for all genes represented by multiple probes on the array and identified as outliers in multiple experimental comparisons (see Additional data file 1). A high degree of expression-ratio reproducibility was observed, even for changes less than twofold, lending confidence to our microarray results and outlier selection criteria. Notably, the 2.0*r* criterion was applied to achieve a high level of stringency in detecting gene outliers. However, this approach precludes the identification of genes that are differentially expressed at levels below 2.0*r* detection (for example, 1.9-fold change) thus obscuring the distinction of tissue-specific outliers and excluding potentially important distinguishing gene cassettes. In the light of this, we compiled a dataset that lists all genes passing the 2.0*r* criterion in at least one experimental comparison and identifies all instances (in other experimental comparisons) where these genes pass a less stringent threshold of 1.2*r* (see Additional data files 2 and 3). Thus, a transcript that shows a minimum change of twofold in one comparison can be subsequently screened for smaller changes, or categorized as having virtually no change in expression (that is, less than 1.2-fold), in other comparisons.

To gauge the accuracy of our methodology in correctly identifying T3-regulated genes, we searched for the 2.0*r* outliers across the three tissues for genes or gene products previously known to be regulated by T3. Representative genes are listed in Additional data file 4 and include 10 genes whose mRNA expression have been reported previously to be regulated by T3 and five genes that are known to be affected by T3 at the protein level. Two genes categorized as effectors are also listed. These include transthyretin (Ttr), a high-affinity serum thyroid-hormone-binding protein that transports thyroid hormone to target tissues, thus facilitating thyroid hor-mone distribution [16], and the retinoid X receptor α (Rxra), a member of the nuclear receptor superfamily that heterodimerizes with TRs and modulates the transcriptional activity of TRs [1].

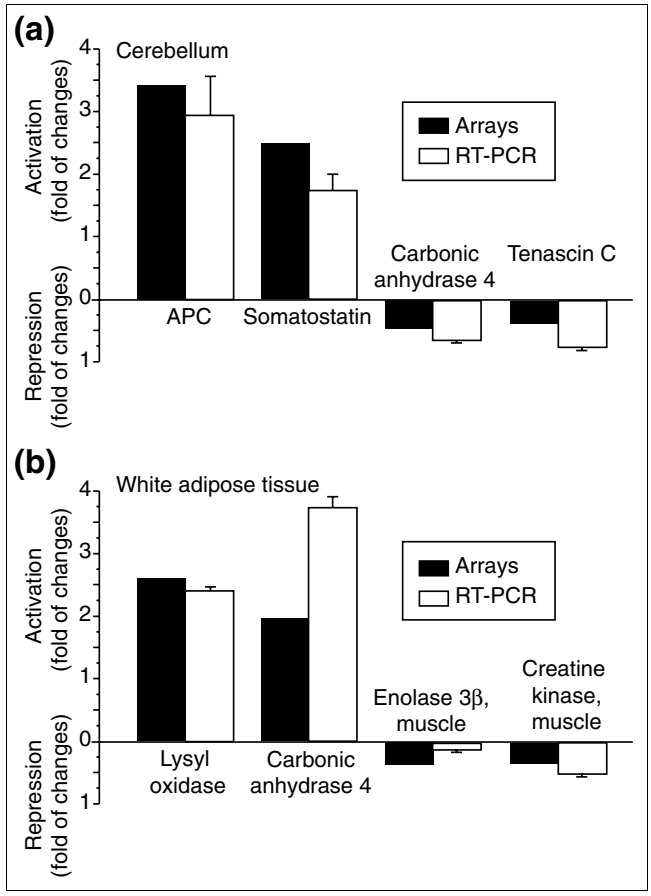

Figure 1
Concordance of gene expression determined by microarrays and RT-PCR. Expression ratios of representative genes in **(a)** cerebellum and **(b)** white adipose tissue identified as outliers by microarrays were determined by RT-PCR as described in Materials and methods. The solid bars represent the data from the microarrays and the open bars are from the RT-PCR (mean ± SEM, $n = 3$).

To confirm the validity of the microarray results, four outliers (two up- and two downregulated genes) each were selected from the cerebellum and WAT for the determination of mRNA expression by reverse transcription PCR (RT-PCR) analysis. The patterns and fold changes in the expression of adenomatous polyposis coli (APC), somatostatin, carbonic anhydrase 4 and tenascin C in the cerebellum (Figure 1a) and those of lysyl oxidase, carbonic anhydrase 4, enolase 3β and creatine kinase in the WAT (Figure 1b) determined by RT-PCR were all consistent with those obtained by the arrays. Even though there was a slight variability in the magnitude of the response between the two methods, the patterns of response were in concordance.

Table 1

Comparison of the numbers of 2.0*r* outliers detected in iT3 and RTH tissues

Condition	Cerebellum			Heart			White adipose		
	Total	Up-regulated	Down-regulated	Total	Up-regulated	Down-regulated	Total	Up-regulated	Down-regulated
iT3	21	18 (86%)	3 (14%)	98	28 (29%)	70 (71%)	58	14 (24%)	44 (76%)
RTH	0	0	0	17	11 (65%)	6 (35%)	172	92 (53%)	80 (47%)

Variability in tissue-dependent transcriptional response in mice treated with T3 and in TRβ$^{PV/PV}$ mice

The number of genes that are differentially expressed in a tissue following T3 treatment can be viewed as an indirect measure of pharmacodynamic effect. For example, tissues that show a large number of gene outliers in response to T3 treatment would suggest higher sensitivity to T3 than tissues responding with a few outliers. This has been found to be true for chemotherapeutic effects, and for estrogen responsiveness [17]. This principle can therefore be used as a metric for assessing tissue sensitivity to T3 treatment or the PV mutant. A breakdown of the number of 2.0*r* outliers identified in each tissue of each comparison is shown in Table 1. The number of outliers varied markedly between tissue types. For example, in the WAT, 58 and 172 outliers were detected in each of the comparisons (that is, with versus without T3 treatment (iT3 mice) and wild-type versus TRβ$^{PV/PV}$ mice (RTH group), respectively), whereas in the cerebellum only 21 were found in the iT3 group and none was found in the RTH group. In the heart, 98 outliers were found in the iT3 group and 17 in the RTH group. Therefore, adult cerebellum appears to be the tissue least sensitive to T3 treatment and the action of PV, whereas the heart is a particularly responsive tissue in our model of hyperthyroidism, and white adipose is the most sensitive tissue in our model of RTH.

Intriguingly, the distribution patterns of up- and downregulated genes showed a consistent trend in two tissues that distinguished the hyperthyroid and RTH conditions (Table 1). In both the heart and WAT, the predominant response to T3 administration (that is, iT3 group) was mostly downregulation of expression (71% and 76% of the outliers, respectively). By contrast, in the TRβ$^{PV/PV}$ mice we observed higher proportions of transcriptionally induced genes. In the heart and WAT of RTH animals, 65% and 53% of outliers, respectively, were upregulated genes. Together, these data support the intriguing view that the hyperthyroid phenotype is largely mediated through T3-induced suppression of gene expression, whereas RTH is underscored by an inappropriate increase in transcriptional activity in T3 target tissues. These data strongly suggest that target-tissue response to T3 administration and the RTH genotype are distinctly different.

To further characterize the target-tissue transcriptional response, we analyzed each tissue for its degree of transcriptional uniqueness. We found that in the T3-treated mice, 24% (5/21), 24% (24/98), and 22% (13/58) of outliers in the cerebellum, heart and WAT, respectively, were tissue specific (that is, differentially expressed by twofold or more in only one tissue, and not more than 1.2-fold in any other tissue). In the RTH mice, 0% (0/0), 53% (9/17), and 47% (81/172) of outliers in the cerebellum, heart and WAT, respectively, were detected in only one tissue type (data not shown). These observations reveal a considerable degree of transcriptional specificity that is dependent on tissue type, consistent with the notion that the transcriptional behavior of TRs depends on the molecular composition of the cell type with respect to the availability and levels of cofactors that modulate TR transcriptional activity [14,18].

Gene classification by transcriptional response

The pathological hallmark of RTH is elevated thyroid hormone associated with nonsuppressible TSH. Even though the phenotypic consequences of elevated thyroid hormone in RTH patients are known, it is not clear what genes mediate the phenotypes. Furthermore, RTH may manifest as hyperthyroidism in one tissue, and, simultaneously, hypothyroidism in another [9]. Dissecting this variable phenotype into the hyperthyroid and non-hyperthyroid components at the molecular level requires a comprehensive knowledge of the hyperthyroid-related genes in each tissue, and the expression patterns of these genes in the context of RTH. Therefore, we performed a tissue-by-tissue analysis cross-comparing the genomic effects of iT3 and RTH to segregate genes according to cognate response patterns.

Four categories of response patterns were discerned and labeled A, B, C and D, as shown in Figure 2. The outliers in category A (brown bars in Figure 2) are the genes that showed the same directionality of change in both T3-treated and TRβ$^{PV/PV}$ mice (that is, up in both or down in both). That the mutant TRβ does not alter the transcriptional response of genes responsive to elevated T3 suggests their potential involvement in the hyperthyroid phenotype. As shown in Figure 2, two genes were identified in the cerebellum, five in the heart, and 39 in the WAT.

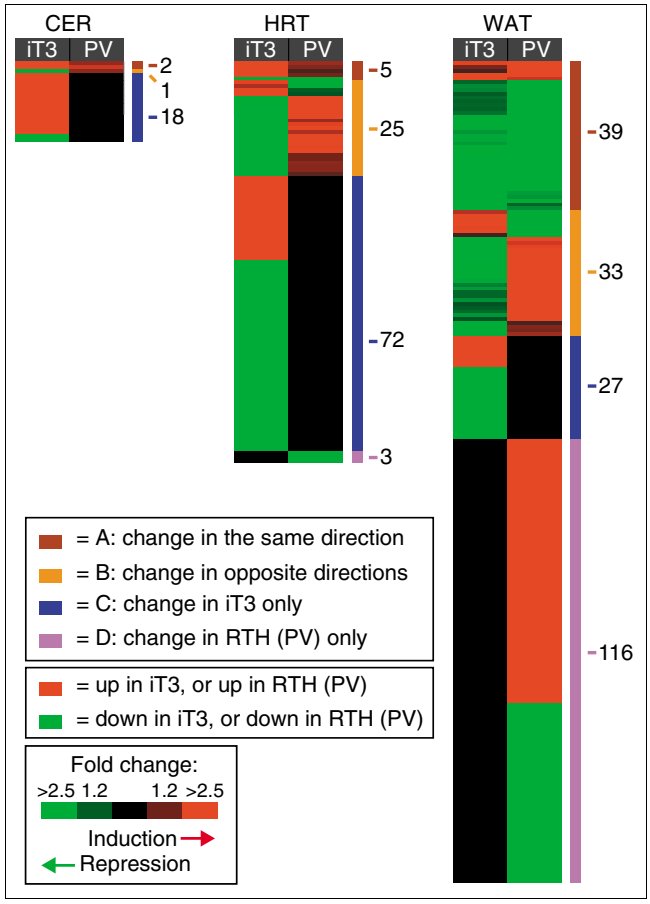

Figure 2
Category analysis of transcriptional response patterns. Intra-tissue expression patterns of genes showing twofold change or more in iT3 and/or RTH (PV) mice are shown. Red indicates higher expression levels in iT3 or RTH mice; green indicates lower expression in iT3 or RTH mice. Black indicates less than 1.2-fold change. The level of color saturation reflects the magnitude of the expression ratio. The number of genes found in each category is shown.

Category B (orange bars) includes the outlier genes that showed reversed patterns of change between iT3 and RTH mice (that is, up in iT3 but down in RTH, or vice versa). Presumably, these genes, which are responsive to increased T3 levels (in iT3 mice), are expressed in the opposite direction in $TR\beta^{PV/PV}$ mice as a consequence of mutant TRβ activity. One such outlier was identified in the cerebellum, 25 in the heart, and 33 in the WAT. Interestingly, 84% (21/25) and 79% (26/33) of these genes in the heart and WAT, respectively, were downregulated in response to T3 treatment and concomitantly upregulated in RTH, further supporting the view that an important molecular aspect of RTH is the abnormal expression of otherwise T3-repressed genes. A mechanistic explanation is that these category B genes are regulated by T3 mostly (or exclusively) through the TRβ receptor.

The majority of the outliers identified in this study, however, were found exclusively in either iT3 (category C, blue bars) or RTH (category D, pink bars) mice. Genes in category C showed a greater than twofold change in iT3 mice and less than 1.2-fold change in RTH mice. Therefore, these genes were responsive to increased T3 in the iT3 group but insensitive to elevated T3 in the presence of the mutant TRβ receptor. In this category, we identified 18, 72 and 27 such genes in the cerebellum, heart and WAT, respectively. Conversely, the outliers in category D were detected in RTH but not in the iT3 group. Compared with category C, a relatively smaller number of such genes were identified in the cerebellum (0 genes) and the heart (3 genes), but a significantly larger number of outliers (116 genes) were detected in the WAT. Taken together, these data show that the expression patterns of iT3 and RTH responsive genes are not only tissue-dependent, but also can differ markedly between the hyperthyroid and RTH states within the same tissue.

Hierarchical clustering identifies biological pathways associated with hyperthyroid (iT3) and RTH phenotypes

Hierarchical clustering of gene-expression patterns can provide a robust, composite view of cellular pathways operative in a biological system as evidenced by the coordinate expression of functionally related genes. To gain insight into the pathways most perturbed in our models, we analyzed the expression patterns of genes differentially expressed in one or more tissues of hyperthyroid (iT3) or RTH mice. In Figure 3, the expression patterns of these genes were hierarchically clustered and the functionality of genes within clusters was analyzed using Gene Ontology (GO) terms. We identified three gene clusters with ostensible biological implications: A, an immunity cluster: B, a lipogenesis cluster; and C, a cell cycle/growth inhibitory cluster. The immunity cluster is largely characterized by a trans-tissue downregulation of genes involved in immune response pathways or immune-cell biology (A, black bar, Figure 3). These genes are repressed in one or more tissues of T3-treated and/or $TR\beta^{PV/PV}$ mice and are all consistently downregulated in the WAT of $TR\beta^{PV/PV}$ mice. These include several HLA class II antigen genes (*H2-Ab1*, *H2-Aa*, and *H2-Eb1*), chemotactic factor genes (*Ccl22* and *Ccl19*), and genes involved in lymphocyte activation (*Lcp2, Ptprcap* and *Ms4a1*) and adherence (*Sell*), strongly suggesting an immunomodulatory response in tissues of both hyperthyroid and $TR\beta^{PV/PV}$ mice.

In the lipogenesis cluster (B, blue bar, Figure 2), six of eight genes have clearly defined roles in fatty-acid and lipid metabolism and include *Fasn*, *Acly*, *Gpd1*, *Elovl6*, *Slc25a1*, and a gene named 'similar to acetyl-coenzyme A carboxylase, clone IMAGE: 5151139' which has 99% identity at the protein level with rat acetyl-coenzyme A carboxylase. These genes are consistently repressed by T3 in the heart and WAT, and expressed at reduced levels in the WAT of $TR\beta^{PV/PV}$ mice, with half of the genes being induced in the heart of $TR\beta^{PV/PV}$ mice (blue bar, Figure 3). These patterns are consistent with the negative regulation of lipogenesis in the hyperthyroid heart

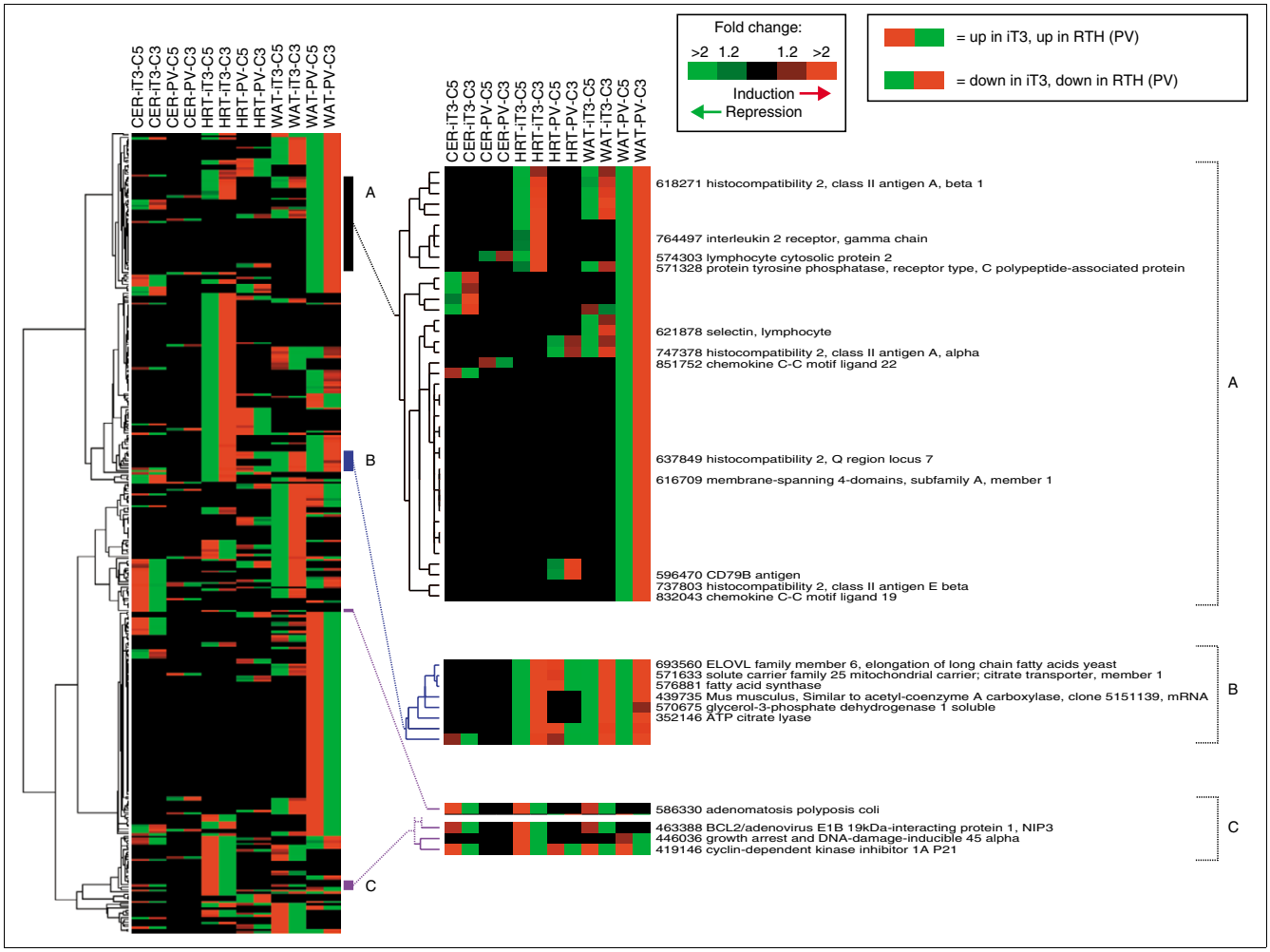

Figure 3
Hierarchical clustering of differentially expressed genes identifies gene clusters with biological associations. Gene-expression patterns are shown in rows; tissue profiles in columns. Degree of color saturation reflects the magnitude of the expression ratio. Note that for optimal clustering, the expression data for each individual dye-swap experiment was used (see key for directionality of expression via color pairs). The black bar at the right side of the main array indicates the immunity cluster, the blue bar the lipogenesis cluster, and purple bars the cell-cycle/growth-inhibitor genes.

and WAT. In RTH mice this suggests suppression of lipogenesis in the WAT with simultaneous increase in lipogenesis in the heart.

The smaller cell-cycle/growth-inhibitory cluster is composed of several genes known to inhibit growth or cell-cycle progression or promote apoptosis (C, pink bars, Figure 3). These genes include *Bnip3*, *Gadd45a* and *Cdkn1a* (*p21*). Shown adjacent to this gene cluster is the similarly expressed gene, *APC* (adenomatous polyposis coli), whose expression is also associated with growth inhibition (that is, via suppression of the Wnt signaling pathway which we recently showed to be negatively regulated by T3 [19]). A hallmark of these genes (with the exception of *Gadd45a*) is increased expression in all three tissues of the hyperthyroid mouse. Notably, *p21* is also upregulated in the heart and WAT of $TR\beta^{PV/PV}$ mice, suggesting its induction in these tissues in response to high circulating T3. These findings raise the possibility that induction of growth-inhibitory mechanisms in multiple T3 target tissues may contribute to the pathogenesis of RTH.

Gene-expression patterns in hyperthyroid and RTH hearts are distinct

The heart is highly sensitive to thyroid hormone and the primary mode of T3 action is a direct influence on cardiac gene expression [20]. Increased heart rate (tachycardia) and myocardial contractility are clinical features common to both hyperthyroidism and RTH [21,22]. As the predominant TR isoform in the heart is TRα1, and RTH patients have normal expression levels of TRα1 together with elevated thyroid hormone, it has been postulated that the cardiac effects common to both hyperthyroidism and RTH are mediated by TRα1 signaling [20,23]. To examine this hypothesis at the molecular level, we compared the genomic effects of induced

Table 2

Gene-expression patterns in iT3 and RTH hearts are distinct

	Heart					
Clone ID and UniGene name	iT3	RTH	Muscle related	Calcium ion binding	ATP binding and electron transport	Mitochondrion related
481408 cytochrome c oxidase, subunit VIIIa	2.78↓	NC			ET	MR
439199 aminolevulinic acid synthase 2, erythroid	3.33↓	NC			ET	MR
571367 BCL2/ adenovirus E1B 19kDa-interacting protein 1, NIP3	3.89↑	1.27↓				MR
350881 RIKEN cDNA 5730438N18 gene	3.73↑	NC				MR
482847 uncoupling protein 3, mitochondrial	3.69↑	NC				MR
318951 malonyl-CoA decarboxylase	2.19↑	NC				MR
920211 solute carrier family 40 (iron-regulated transporter), member 1	2.13↑	NC				MR
571633 solute carrier family 25 (mitochondrial carrier; citrate transporter), member 1	3.03↓	1.38↑				MR
318134 translocator of inner mitochondrial membrane a	3.13↓	NC				MR
481469 [Mrps18b]	4.00↓	NC				MR
423605 aldehyde dehydrogenase 1 family, member B1	3.45↓	NC			ATPB	MR
352146 ATP citrate lyase	2.78↓	NC			ATPB	
570675 glycerol-3-phosphate dehydrogenase 1 (soluble)	3.33↓	NC			ATPB	
554335 Rous sarcoma oncogene	5.00↓	NC			ATPB	
1196244 lymphocyte protein tyrosine kinase	7.69↓	NC			ATPB	

Table 2 *(Continued)*

Gene-expression patterns in iT3 and RTH hearts are distinct					
349954 myosin heavy chain 11, smooth muscle	2.04↓	NC	MC		ATPB
318692 sarcolipin	4.76↓	3.58↑	MC		
604414 (vimentin)	2.56↓	2.27↑	MD		
890932 calcium channel, voltage-dependent, alpha2/delta subunit 1	2.10↑	NC	MC	CCA	
479382 myosin light chain, regulatory A	20.0↓	6.64↑	MC	CIB	
354796 fibulin 1	2.38↓	NC		CIB	
472672 S100 calcium binding protein A10 (calpactin)	2.70↓	NC		CIB	
335868 (angiotensinogen)	3.13↓	NC		CIB	

↑ indicates fold of activation; ↓ indicates fold of repression; NC indicates no changes (< 1.2-fold). MC, muscle contraction; MD, muscle development; CCA, calcium channel activity; CIB, calcium ion binding; ATPB, ATP binding; ET, electron transport; MR, mitochondrion related.

hyperthyroidism and RTH in the mouse heart. In total, we identified 105 gene outliers that showed twofold change or more in the iT3 or RTH groups (see Additional data file 5). Notably, this list does not include several genes previously implicated in T3-mediated cardiac effects such as those for the α- and β-myosin heavy chains, *SERCA2* and *HCN2*, as they were not represented on our microarray. To focus on the set of most relevant genes in our list, we used the GO database of biological and functional gene classifications [24] to define genes known or expected to have a role in cardiac muscle contraction.

Hence, we classified 23 genes into one or more of the following categories (Table 2): muscle-related; calcium-ion binding (calcium-ion release and retrieval is central to muscle contraction and relaxation); ATP binding and electron transport (ATP is the immediate source of energy that powers muscle contraction); mitochondrion related (cardiac muscle has the richest supply of mitochondria and T3 directly boosts energy metabolism in mitochondria via gene transcription).

We hypothesized that the expression patterns of these genes would be similar in the iT3 and RTH hearts as they are presumably regulated by TRα1 and responsive in the context of elevated T3. Surprisingly, however, this analysis indicated that the iT3 and RTH hearts are molecularly distinct. Of the 23 genes identified, none showed the same or similar response patterns. Eighteen genes, which ranged from four-fold induction to 20-fold suppression in the iT3 heart, showed less than a 1.2-fold change in RTH (that is, category C genes, Figure 2). Moreover, the remaining five genes were expressed in opposite directions (that is, category B genes, Figure 2). These include the gene for myosin light chain, regulatory A (> 20-fold repressed in iT3 and > 6.6-fold increased in RTH) and the sarcolipin gene (> 4.8-fold repressed in iT3 and > 3.6-fold increased in RTH).

This expression pattern trend was also apparent in the remaining 82 non-muscle-contraction-related outliers (see Additional data file 5). Of these genes, 54 showed from 2- to 11-fold change in response to T3 injection and concurrently no change in RTH mice, while only three showed a greater then twofold change in RTH with no concurrent change in iT3 mice. Of the 25 genes in this group that showed change in both iT3 and RTH mice, only five showed change in the same direction (that is, candidates for TRα1-dependent transcription, category A genes, Figure 2), whereas the remaining 20 genes showed opposing expression patterns. Such marked differences between iT3 and RTH hearts suggest a greater role for TRβ in the heart than previously envisioned, or interference of TRα1-mediated transcription by TRβPV or its downstream effects.

Functional interpretation of expression profiles in the WAT of RTH mice

Thyroid hormone is an important regulator of adipose tissue development and metabolism. T3 is thought to exert its effects on fat cells through transcriptional regulation by both α1 and β receptors [25]. Although a number of T3 target genes in adipose tissues have been described [26,27], little is known of the transcriptional response of adipocyte T3 target genes in RTH. Accordingly, we compared WAT expression patterns in the iT3 and RTH groups. In total, we identified 215 genes that showed twofold change or more in either iT3 or RTH (see

Table 3

Genes involved in cell adhesion, lipogenesis and immune cell biology are modulated in white adipose tissue of RTH and iT3 mice

	WAT	
Clone ID and UniGene name	iT3	RTH
Cell Communication: cell adhesion		
484261 : keratin complex 1, acidic, gene 13	NC	2.36↑
335736 : keratin complex 2, basic, gene 6a	NC	2.73↑
464060 : keratin complex 1, acidic, gene 19	NC	3.54↑
420709 : RIKEN cDNA 5730453H04 gene	NC	14.02↑
762299 : CEA-related cell adhesion molecule 1	NC	4.87↑
776133 : cadherin 1	NC	6.20↑
719965 : desmocollin 2	NC	2.79↑
761578 : desmoglein 2	1.49↓	3.30↑
Metabolism: lipogenesis		
570675 : glycerol-3-phosphate dehydrogenase 1 (soluble)	2.33↓	1.49↓
352146 : ATP citrate lyase	4.17↓	2.94↓
439735 : Mus musculus, Similar to acetyl-coenzyme A carboxylase, clone 5151139	2.13↓	2.38↓
576881 : fatty acid synthase	2.94↓	3.13↓
693560 : ELOVL family member 6, elongation of long chain fatty acids (yeast)	2.38↓	2.22↓
578436 : phosphogluconate dehydrogenase	1.72↓	3.03↓
949810 : hexose-6-phosphate dehydrogenase (glucose 1-dehydrogenase)		2.50↓
Response to external stimuli: immune cell biology		
620268 : CD53 antigen	2.27↓	2.86↓
621878 : selectin, lymphocyte	1.33↓	2.44↓
618271 : histocompatibility 2, class II antigen A, beta 1	1.30↓	3.02↓
747378 : histocompatibility 2, class II antigen A, alpha	1.43↓	4.55↓
597433 : chemokine (C-X-C motif) ligand 13	1.27↓	2.44↓
637849 : histocompatibility 2, Q region locus 7	NC	2.27↓
748587 : histocompatibility 2, class II antigen E beta	NC	2.70↓
575397 : chemokine (C-C motif) ligand 6	NC	2.13↓
851752 : chemokine (C-C motif) ligand 22	NC	3.02↓
832043 : chemokine (C-C motif) ligand 19	NC	2.78↓
596470 : CD79B antigen	NC	2.94↓

↑ indicates fold of activation; ↓ indicates fold of repression; NC indicates no changes (< 1.2-fold).

complete list in Additional data file 6). Assignment of the named genes to GO biological processes (tier 3) revealed four predominant biological classes: metabolism (n = 45), cell growth and maintenance (n = 24), cell communication (n = 24) and response to external stimuli (n = 16). The expression patterns of genes in these categories provide a molecular framework for interpreting the biological properties of WAT in RTH. The length limitation of this paper permits only description of a selected subset of genes. For example, within the cell communication class we identified a number of genes upregulated in RTH that are involved in cell-cell adhesion via desmosomal junctions (Table 3). Desmosomes are major intercellular adhesive junctions that provide strong mechanical attachments between adjacent cells and are thought to have a role in tissue morphogenesis and differentiation [28]. The adhesive core of the desmosome is comprised of proteins of the cadherin family, namely desmogleins and desmocollins. In the WAT of RTH animals, we observed a marked upregulation of transcript levels of cadherin 1, desmoglein 2, desmocollin 2 and the CEA-related cell adhesion molecule 1. Desmosomes are anchored to intermediate filaments of keratin in the cytoplasm. Here, we also observed increased transcript levels of the keratins Krt1-13, Krt1-19 and Krt2-6a. In addition, the most highly upregulated transcript in the WAT of RTH mice was a gene called 5730453H04Rik, which shares 95% identity (over 480 amino acids) with human desmoplakin, a major protein of desmosomes involved in the anchoring of keratin intermediate filaments to desmosomes.

Within the metabolism class, we identified a number of genes negatively regulated in the WAT of iT3 and RTH mice that are directly involved in fatty-acid and lipid metabolism (Table 3). These genes include those previously discovered in the lipogenesis cluster of Figure 3 (that is, *Fasn*, *Acly*, *Gpd1*, *Elovl6*, *Slc25a1* and IMAGE: 5151139). Fatty-acid biosynthesis is known to use large amounts of NADPH. As a consequence, adipose tissue is known to express high levels of the enzymes of the pentose phosphate pathway that generate NADPH. Hexose-6-phosphate dehydrogenase and phosphogluconate dehydrogenase are two of the three major enzymes in the pentose phosphate pathway, and both were negatively regulated in the WAT of RTH animals.

The genes assigned to the class response to external stimuli were, with only one exception, all downregulated in RTH animals, and in some cases, in iT3 mice (Table 3). All the genes identified here are involved in immune response or immune-cell biology and overlap with the previously identified immunity-gene cluster of Figure 3. They include a number of chemokines, HLA antigens and other markers of lymphoid lineages.

Taken together, these data suggest that the WAT of RTH mice is characterized by increased cell-cell adhesion via desmosomal structures, and they recapitulate our initial findings of a possible hyperthyroid-associated inhibition of lipogenesis and a repression of immunomodulatory signaling.

Gene-expression patterns in the cerebellum of iT3 and RTH mice

Thyroid hormones are essential for normal brain development and regulate neuronal proliferation, migration and synaptogenesis in the cerebellum [29,30]. In our study, the cerebellum was the least responsive tissue in both iT3 and RTH mice, with only 13 genes and no genes, respectively showing twofold or greater changes. The complete list of genes with all GO classifications is shown in Additional data file 7. The most highly induced gene (> threefold) in the cerebellum of T3-treated mice was the T3/T4-binding protein, transthyretin, which is synthesized in large amounts in the choroid plexus and is essential for the transport of thyroid hormones from the blood to the brain [31]. Increased expression of transthyretin may represent a positive feedback mechanism for enhancing the effect of thyroid hormone in the brain. mRNA for the retinoid X receptor (RXR) was also induced more than threefold in response to T3. RXR is a member of the nuclear receptor superfamily that heterodimerizes with TRs and modulates the transcriptional activity of TRs [1]. T3-induced upregulation of RXR may reflect the relative importance of TR-RXR heterodimerization for T3 action in the cerebellum. Also induced by T3 treatment were the genes *APC* and *dickkopf homolog 3*, which are known or suspected antagonists of the Wnt signaling pathway. Both T3 and Wnt pathways are known to have important roles in neuronal growth and synaptogenesis [32-35]. We recently presented genetic and biochemical evidence that thyroid hormone can inhibit the Wnt signaling pathway [19]. Thus, T3-mediated inhibition of Wnt signaling may be an important aspect of cerebellar development and function. The physiologic impact of the activation of these genes in hyperthyroidism warrants further investigation.

Discussion

In this study, we sought to define the molecular basis of the target-tissue phenotype for hereditary TRβ mutations using a global gene expression approach. Specifically, we used expression profiling as a complex readout for the *in vivo* actions of T3 and PV in target tissues. The animal model was a murine line with the TRβ disrupted in the identical manner as found in the human condition (TRβPV mice). This TRβPV mouse faithfully reproduces human RTH [11,13,14]. To study the *in vivo* effects of T3 in the presence of normal TRβ, we used a mouse model of pharmacologic hyperthyroidism by treating the wild-type siblings with T3 (iT3 mice). This model aided in the delineation of genes associated with the hyperthyroid and RTH phenotype. Gene-expression patterns were analyzed in three T3 target tissues - cerebellum, heart and WAT - previously shown to have marked variation in metabolic patterns after T3 treatment.

Several interesting observations emerged from our study. First, we found that the normal physiologic effect of T3 on specific tissues is predominantly downregulation of gene expression. In the T3-treated mice, the majority of expression outliers in the heart (71%) and WAT (76%) were repressed. The same phenomenon has been observed in other mouse *in vivo* expression studies, albeit using less comprehensive array technologies. Feng *et al.* [36] identified 55 outliers in the livers of hypothyroid mice injected with T3; of these, 14 (25%) were upregulated and 41 (75%) were downregulated. Similarly, in a mouse model of T3-induced involution of a thyrotrope tumor, Wood *et al.* [37] identified 47 T3-responsive genes: seven (15%) were upregulated whereas 40 (85%) were downregulated. Thus, taken together, these studies indicate that T3 predominantly suppresses gene expression in responsive tissues. As would be predicted, in the RTH model, the majority of genes in the heart (63%) and, to a lesser extent in the WAT (53%), were upregulated. Of the 25 genes in the heart and 33 genes in WAT that showed opposite expression patterns in RTH (PV) and iT3 mice, 84% and 79% in heart and WAT, respectively, were repressed by T3 treatment and induced in RTH. Together, these data suggest that certain RTH (and perhaps hypothyroid) tissue phenotypes may be due predominantly to the inappropriate induction of genes normally repressed by T3. Using the number of differentially expressed genes as a semi-quantitative measure of pharmacodynamic effect, we found that the cerebellum is by far the least responsive in both iT3 and RTH, whereas the heart is the most responsive in iT3 (approximately fivefold more than cerebellum and approximately twofold more than WAT; Table 1) and the WAT is the most responsive in RTH (around 10-fold more than heart, while the cerebellum showed no changes in gene expression greater than twofold; Table 1).

Category analysis of expression patterns in iT3 and RTH mice shed light on the transcriptional consequences of the PV mutant (Figure 2). Category A consists of genes for which the T3-induced response was not affected by the expression of PV, indicating that the responses of these genes to increased T3 are likely to be exclusively mediated by TRα1. However, we have recently demonstrated that PV can form inactive heterodimers with TRα1, thereby suppressing the transcriptional activity of TRα1 [10]. This suggests the possibility that genes in category A may, in some instances, be modulated by TR-independent pathways: a notion supported by recent studies demonstrating that T3 can act in alternate pathways independent of TRs [38]. Categories B and C consist of T3-response genes mediated by TRs, but their transcriptional responses are altered by PV. In category B, the directionality of response in iT3 and RTH is reversed. These genes may be of particular importance in the phenotypic manifestations of RTH. Notable examples are the TSHβ and the α-glycoprotein common subunit genes that are repressed in the mouse pituitary following T3 administration [39]. However, in the pituitary of $TR\beta^{PV/PV}$ mice, the expression of the PV mutant leads to the induction of these two genes, resulting in the highly elevated serum TSH [11].

Genes in category C were responsive to T3 treatment yet insensitive to hyperthyroid levels of T3 in the presence of PV. These genes are not differentially expressed between untreated euthyroid wild-type mice and $TR\beta^{PV/PV}$ littermates and thus may reflect changes specific to pharmacologic hyperthyroidism. Alternatively, these genes may be primary targets of TRα1 and their expression levels in $TR\beta^{PV/PV}$ mice mimic euthyroid levels as a result of partial transcriptional interference by PV. Some of the interesting genes in this category include cytochrome *c* oxidase, subunit VIII and Rous sarcoma oncogene (Table 2).

One particularly interesting finding concerns the genes in category D. These genes did not respond to T3 treatment, but showed altered expression in the presence of PV. WAT had a particularly high number of genes in this category (53% (116/215) compared to heart (3%) (3/105)). The modulation of these genes in RTH could arise from the systemic effects of T3 resistance. Alternatively, the transcriptional response of these genes could be mediated by PV, either directly or indirectly, in a T3-independent manner. For example, we have previously shown that PV can heterodimerize with the 9-*cis* retinoacid receptor, RXR [10]. Heterodimerization of a mutant TRα with other nuclear receptors could simultaneously alter other hormone signaling pathways in RTH in a T3-independent manner.

The experimental design of this study afforded a unique opportunity to investigate the involvement of cellular pathways that may contribute to the pathophysiology of mutant TRβ action in the intact animal. Through pattern analysis of genes identified as differentially expressed in iT3 or $TR\beta^{PV/PV}$ mice in one or more tissues, we identified several gene clusters with clear functional associations that may have pathological implications in thyroid hormone disease (Figure 1). Then, on a tissue-by-tissue basis, we were able to focus on expression patterns and pathways most relevant to the tissue type.

The lipogenesis cluster in Figure 3 consists of six genes (*Fasn*, *Acly*, *Gpd1*, *Elovl6*, *Slc25a1* and the homolog of rat *Acac*) that were repressed in both iT3 and RTH mice (category A genes; Table 1). These genes are known to have important roles in fatty-acid and lipid synthesis. This finding presumably reflects the known function of T3 as a regulator of lipogenesis and lipolysis in adipocytes [26] and, specifically, as a transcriptional modulator of *Fasn*, *Acly* and *Gpd1* [40-42]. Whereas T3 is known to induce lipogenesis in the liver [26], downregulation of fatty-acid synthase and acetyl-CoA carboxylase genes was reported in brown adipose tissue of T3-treated hypothyroid rats [24]. This is consistent with the physiologic findings that hyperthyroid rats display diminished fatty-acid synthesis in brown and white adipose tissues

[26]. That all six of these genes were downregulated in the WAT of both iT3 and RTH mice suggests that the T3-mediated inhibition of lipogenesis in this tissue is independent of TRβ and may be the main targets of TRα1 in this tissue. This possibility is supported by the observations of multiple TR transcriptional response elements in the promoters of both *Fas* and *Gpd1* [43,44] and the observation that mice heterozygous for a TRα1 point mutation (resulting in a dominant-negative TRα1 mutant with elevated T3 and T4) showed a more than fourfold increase in body fat compared to wild-type mice [45]. The suppression of these genes in both T3-treated and $TR\beta^{PV/PV}$ mice could represent an important mechanism in the phenotype of body-fat reduction common to both hyperthyroidism and RTH.

We identified in Figure 3 a small cluster of genes with similar expression patterns that are composed of cell-cycle inhibitory and apoptosis-promoting genes. *Cdkn1a* (encoding p21, a major cyclin-dependent kinase inhibitor that induces G1 arrest), *APC* (a negative regulator of Wnt-induced cell proliferation), and *Bnip3* (a potent promoter of apoptosis) are all induced by T3 treatment in the cerebellum, heart and WAT. The gene for the growth inhibitor Gadd45a is induced in the heart of iT3 mice and the WAT of RTH mice, in a fashion similar to that of *Cdkn1a*. Though the mitogenic activity of thyroid hormone has been documented *in vitro* [46,47], little is known of the cellular mechanisms underlying the antiproliferative [48,49] and apoptotic effects [50,51] of T3. Recently, we and others have shown that T3 treatment of cultured cells can induce expression of the *p53* tumor suppressor gene [19,52]. Several of the genes in this T3-inducible cluster are known transcriptional targets of p53, including *Gadd45a* [53], *Cdkn1a* [54] and *APC* [55], suggesting that a coordinated transcriptional cassette supportive of growth arrest induced by T3 is likely to be mediated directly and/or indirectly by TRα1. The induction of an antiproliferative/tumor suppressor pathway is also consistent with our previous findings that the Wnt pathway is coordinately repressed by T3 in rat pituitary cells [19]. v-*erbA* is a viral oncogene whose oncogenic function is the inhibition of the thyroid hormone receptor through a dominant-negative effect. These observations support our hypothesis that a major mechanism for the transforming function of v-*erbA* is its cellular inhibition of T3/TRα1 effects, resulting in coordinate upregulation of oncogenic pathways (that is, the Wnt signaling pathway), and repression of antiproliferation and tumor suppressor signals (for example, p53, Gadd45a, Cdkn1a).

Finally, we discovered an overall repression in the expression of immune-related genes in iT3 and RTH mice (Figure 3). To further understand the functions of these genes, we analyzed the expression of all outlier genes from the Figure 3 dataset with known roles in immune response or immune-cell biology. The expression profiles of 28 genes meeting these criteria are shown in Figure 4. Interestingly, all but six of these 28 genes showed reduced expression in the WAT of $TR\beta^{PV/PV}$ mice, and half were repressed in the hearts of iT3 mice. That these genes represent lineage-specific markers of a variety of immune cells, and that they are consistently reduced in two tissues (the heart (iT3) and WAT (RTH)), suggests that at least a fraction of these genes may reflect a general lack of lymphocytes in these tissues of hyperthyroid and RTH mice. Indeed, it has been observed that hypothyroid mouse strains have significantly reduced numbers of pro-B, pre-B, and B cells, and treatment of these mice with T4 increases the number of B-lineage cells [56]. In addition, increases in numbers of splenic and thymic T cells and splenic NK cells have also been observed in mice treated long term with T3 [57]. Intriguingly, mouse primary adipocytes themselves are known to be capable of expressing multiple chemokines and inflammatory mediators [58]. As shown in Figure 4, we also observed reduced expression of chemokines CCL22, CCL6 and CXCL13 (which together are chemotactic for B cells, T cells, monocytes and macrophages) and induction of Socs5 (a suppressor of cytokine signaling) in the WAT of RTH mice. The repression of these genes could contribute to an attenuation of lymphocytic residence in this tissue.

The heart is a major target of thyroid hormone action, and T3 has a direct effect on heart rate and contractile function. Both TRα1 and TRβ are expressed in cardiac myocytes; however, TRα1 is the predominant subtype, and recent reports have suggested a primary role for TRα1 in mediating T3 effects in the heart [10,59,60]. It has been hypothesized that, in cardiac tissue from $TR\beta^{PV/PV}$ mice, the primary effects of the elevated T3 would be mediated through heightened T3/TRα1 signaling and that the expression response would be similar, if not identical, to that found in the myocardium of wild-type mice with induced hyperthyroidism by exogenous administration of T3. Contrary to this hypothesis, we observed a large degree of discordant cardiac gene expression when we compared the responsive genes of T3-treated animals having wild-type TRα1 and TRβ with those of $TR\beta^{PV/PV}$ mice with wild-type TRα1 (Table 2). The hearts of T3-treated animals showed expression of genes indicative of an altered workload. When heart workload increases or decreases, there is a switch in energy source from predominantly the oxidation of fatty acids to the oxidation of glucose [61]. Three key regulators facilitate this switch: malonyl-CoA decarboxylase (MCD), uncoupling protein 3 (UCP3) and pyruvate dehydrogenase kinase 4 (PDK4). In our study, both MCD (which regulates β-oxidation of long-chain fatty acids) and UCP3 (which uncouples the oxidative phosphorylation of ADP) were upregulated at the mRNA level in the hearts of T3-treated animals, with concommitant downregulation of all the genes of the lipogenesis cluster (Figure 3). In contrast, the RTH heart did not show induction of MCD or UCP3, but rather shows increased mRNA levels for the lipogenic genes *Fasn*, *Elovl6* and *Slc25a1*, suggesting a different metabolic signaling in the RTH heart. Recently, Swanson *et al*. reported that the $TR\beta^{PV/PV}$ mice, under euthyroid conditions, have decreased heart rate and contractile function, demonstrating that despite a

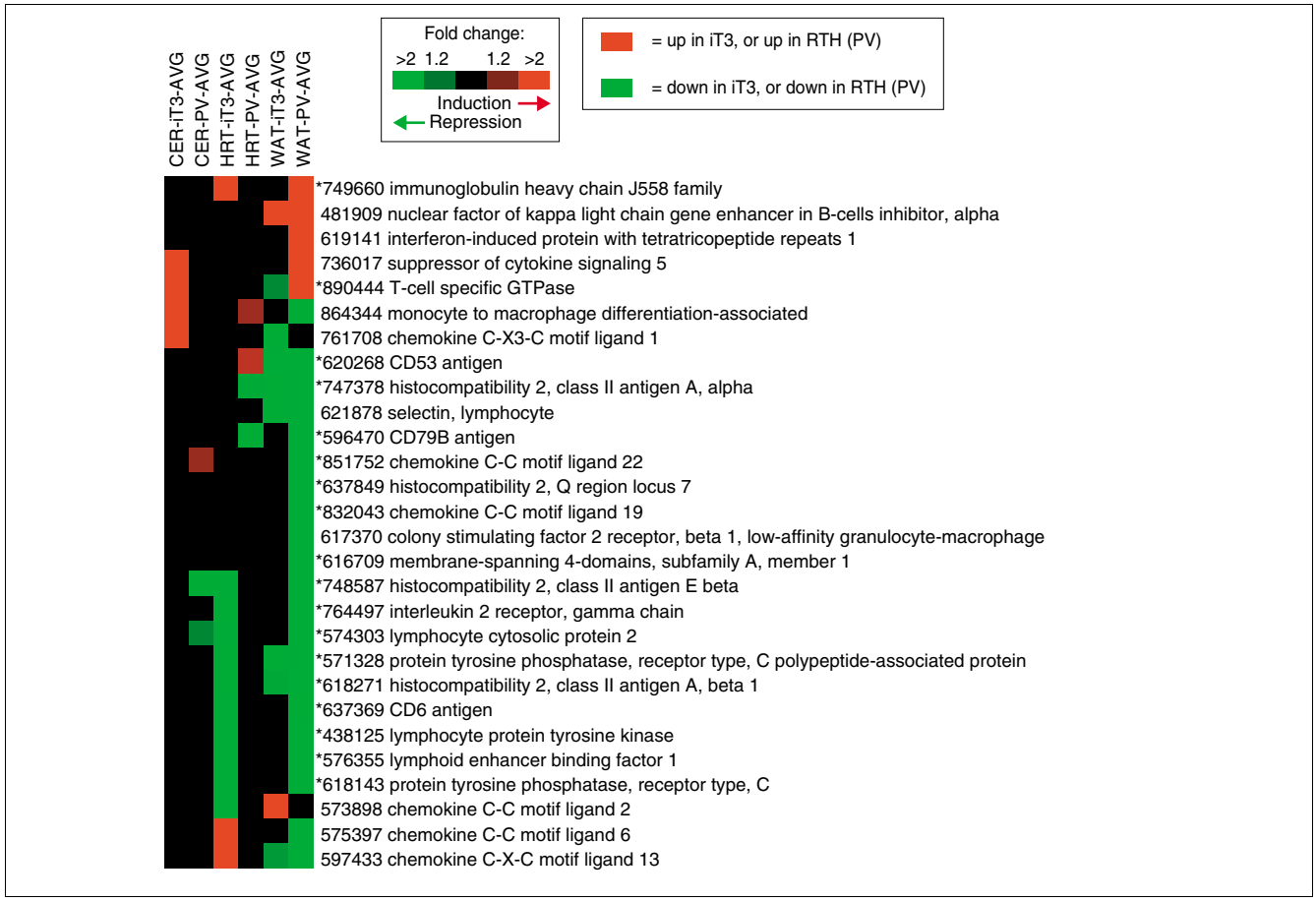

Figure 4
Treeview visualization of iT3- and PV-responsive immunity/lymphocyte-related genes. Higher and lower transcript levels in T3-treated animals (iT3) or RTH mice (PV) are indicated by arrows (as relative to iT3 control or wild-type mice, respectively). IMAGE clone IDs and UniGene names are given; asterisks (*) indicate immune cell-specific genes.

lower expression of TRβ as compared with TRα1 in the mouse heart, the homozygous PV mutant can negatively interfere with TRα1 signaling in this organ [62]. Our genomic results are in agreement with these physiologic findings and provide a glimpse at the gene-by-gene tissue response to T3 stress.

Conclusions

The clinical manifestations of RTH and hyperthyroidism are well documented, and although the genetic cause of RTH is known, the target-tissue transcriptional responses and cellular pathways affected are far from being understood. In our study we have used expression profiling to dissect the molecular consequences of a dominant-negative TRβ homozygous mutation *in vivo*, and in the process, develop a better understanding of TRα1 effects in the whole animal. Our results show that T3 primarily acts to repress gene expression, and that TRβ has a greater modulating effect in the heart than originally thought. Moreover, we identified novel physiologic candidates for more subtle T3 action such as changes in immune-gene expression, and in the induction of antiproliferative genes. Lastly, our analysis further confirms that the relative levels of TR isoforms lead to dramatic differential effects on gene expression. The results permit the identification of genetic elements that contribute to downstream isoform effects in individual tissues [59,60].

Materials and methods

Mouse strains and treatment

The animal protocols used in the present study have been approved by the National Cancer Institute Animal Care and Use Committee. The TRβPV mice contain a cytosine insertion in exon 10 of the TRβ1 gene at nucleotide position 1,642 of the TRβ1 cDNA. This mutation leads to a frameshift of the carboxy-terminal 14 amino acids of TRβ1 [11,12]. TRβPV mice were prepared via homologous recombination and maintained on a mixed background of 129/Sv × C57BL/6J [11]. $TR\beta^{+/+}$ and $TR\beta^{PV/PV}$ male siblings at 8-10 weeks of age were used in this study. Another group of wild-type ($TR\beta^{+/+}$) male

littermates of $TR\beta^{PV/PV}$ received daily intraperitoneal injections of T3 (5 μg/mouse) or the same volume of vehicle (phosphate-buffered saline) for 7 days. On the eighth day the animals were sacrificed by CO_2 exposure and tissues (cerebellum, heart and white adipose) were harvested.

RNA preparation

Total RNAs were extracted from liquid nitrogen-frozen tissue specimens using Trizol reagent according to the manufacturer's instructions (Gibco-BRL). To minimize differences in gene expression owing to inter-animal variability, for each tissue and animal category, 5 μg of total RNA from four animals were pooled before RNA amplification. RNA amplification and quality assessment was carried out as previously described [64].

Microarray design and manufacture

The mouse cDNA microarrays contained 11,520 sequences derived from various sequence-verified clone collections including the Incyte GEM1 mouse clone set (8,700; Incyte), the Research Genetics mouse sequence-verified set (2,600; Research Genetics,), and a private collection of 200 mouse ESTs (a gift from Lothar Heninghausen, NCI, Bethesda, MD). All arrays were manufactured at the NCI Microarray Facility at the Advanced Technology Center, Gaithersburg, MD. Arrays were printed using an OmniGrid microarrayer (GeneMachines) on poly-L-lysine-coated-glass according to Eisen and Brown [63].

Microarray hybridization and scanning

For each experimental comparison, duplicate microarray hybridizations were performed according to a reciprocal strategy termed dye-swapping. In this approach, the Cy3 and Cy5 labeling scheme for the two arrays are reversed such that a true differentially expressed gene having a ratio of 2.0 (that is, a 2-fold red (Cy5-biased) spot) on one array, for example, would have a reciprocal ratio of approximately 0.5 (that is, a 2-fold green (Cy3-biased) spot) on the other array. Notably, this form of experimental replication is more rigorous than conventional duplication (that is, true replicates using the same labeling scheme) as it takes into account a recognized form of experimental noise in microarray technology characterized by the reproducible bias of one fluorophore over the other at low signal intensity features (termed dye bias). Three micrograms amplified RNA were used to generate Cy3- or Cy5-labeled cDNA for each array hybridization. cDNA labeling reaction and array hybridization were carried out essentially as described [63]. Microarrays were scanned on a GenePix 4000A microarray scanner (Axon Instruments) to generate 16-bit TIFF images of Cy3 and Cy5 signal intensities. The images were analyzed using GenePix Pro 3.0 microarray analysis software to measure fluorescence signals and format data for database deposition.

Outlier selection and data analysis

All array data were deposited in the NCI-CIT microarray database [65] where Cy3 and Cy5 signals were median normalized and expression ratios (Cy5/Cy3) were calculated. The following selection criteria were applied. All spots having a mean signal (after background subtraction) less than twice that of background in both Cy3 and Cy5 channels were systematically excluded from the dataset to eliminate measurements based on poorly detected features. The data were also filtered to exclude spots flagged as missing or corrupt in one or both arrays of a dye-swap pair. Remaining outliers were then selected by the 2.0*r* criterion, whereby an expression ratio must demonstrate a twofold or greater change on each array of a pair of reciprocal dye-swap hybridizations. We also demanded that the ratios must be in opposite expression directions (that is, > 2.0 on one array, and < 0.5 on the other) to exclude 'false-positive outliers' that showed a reproducible bias towards either red or green fluorescence and thus failed to reciprocate in the dye-swap array pairs. We next calculated the average expression ratio from the dye-swap pairs (after taking the reciprocal ratio from one of the two arrays) and report the average expression ratios in all analyses herein. For reporting genes by name, IMAGE clone IDs corresponding to the microarray probe sequences were used to extract UniGene Cluster IDs and names (UniGene Build 129). For genes represented by multiple probes on the array, a single probe was used (that is, the probe that showed the greatest transcriptional variation) to report the expression ratio so as to prevent gene number biasing owing to redundant probes.

RT-PCR analysis

The expression of selected genes was also analyzed by quantitative RT-PCR using the following pairs of primers:

APC forward primer 5'-GCTGACATCTGTGCTGTGGATGG-3';

APC reverse primer 5'-TCCTTAAAGCTGCTGCACTTCCC-3';

somatostatin forward primer 5'-TGCATCGTCCT-GGCTTTGG-3';

somatostatin reverse primer 5'-GAGTTAAGGAAGAGATAT-GGG-3';

tenascin C forward primer 5'-TTCGTGTGTTCGCCATCTTG-3';

tenascin C reverse primer 5'-GTGTGAGGTCGATGGTGGT-3';

carbonic anhydrase 4 forward primer 5'-TCACTGCTAG-GACAAAGGTG-3';

carbonic anhydrase 4 reverse primer 5'-AGAGGTTGAAT-GGGGTTTGG-3';

lysyl oxidase forward primer 5'-CTACATCCAGGCTTCCACG-3';

lysyl oxidase reverse primer 5'-TCTCCTCTGTGTGTT-GGCAT-3';

enolase 3β, muscle forward primer 5'-TCAAGGGTTA-CACTCTGCCT-3';

enolase 3β, muscle reverse primer 5'-TCGTTCAC-CCACACAAGGAA-3';

creatine kinase, muscle forward primer 5'-TTCCTTGTGT-GGGTGAACGA-3';

creatine kinase, muscle reverse primer 5'-TTTTCCAGCTTCT-TCTCCATC-3';

GAPDH forward primer 5'-ACATCATCCCTGCATCCACT-3';

GAPDH reverse primer 5'-GTCCTCAGTGAGCCCAAG-3'.

Total RNA (5 μg) prepared as described above was used in the quantitative RT-PCR reaction. cDNA was prepared by SuperScript II reverse transcriptase I (Invitrogen) in the presence of poly(dT) primer. Preliminary experiments were carried out to define the conditions under which the amplification by PCR was in the linear range. The final conditions used for each were: 94°C for 30 sec, 60°C for 30 sec, 72°C for 30 sec followed by 72°C for 2 min. A total of 26 cycles were used for the amplification of APC, carbonic anhydrase 4, lysyl oxidase and somatostatin cDNA. A total of 32 cycles were used for the amplification of tenascin C, enolase 3β (muscle) and creatine kinase (muscle) cDNA. The PCR products were analyzed by 2% agarose gel electrophoresis and detected by ethidium bromide staining. The intensities of the bands were quantified by Eagle Eye (Stratagene). The expression of GAPDH was determined similarly (22 cycles) as an internal control. The band intensities of the quest genes were normalized against the control. The data are expressed as mean value ± SEM (n = 3 independent determinations). Differences between groups were examined for statistical significance using Student's t-test. $p < 0.05$ is considered statistically significant.

Additional data files

The following additional data files are available with the online version of this article and also at the authors' website [66]: an Excel table (Additional data file 1) of all redundant microarray probes and their average expression ratio measurements; an Excel file (Additional data file 2) containing a comprehensive filtered gene list of average expression ratios; a figure (Additional data file 3) showing a hierarchical clustergram of 2.0*r* outlier genes with full annotation; a Word table (Additional data file 4) listing the responsive genes known to be modulated by T3; an Excel table (Additional data file 5) listing genes differentially expressed in the heart of iT3 and/or RTH mice, while another table (Additional data file 6) lists genes differentially expressed in the white adipose tissue (WAT) of iT3 and/or RTH mice. Also provided is an Excel file (Additional data file 7) listing genes that are differentially expressed in the cerebellum of iT3 and/or RTH mice; and, finally, a zipped text file (Additional data file 8) containing the raw data.

References

1. Cheng SY: **Multiple mechanisms for regulation of the transcriptional activity of thyroid hormone receptors.** *Rev Endocr Metab Disord* 2000, **1:**9-18.
2. Yen PM: **Physiological and molecular basis of thyroid hormone action.** *Physiol Rev* 2001, **81:**1097-1142.
3. Harvey CB, Williams GR: **Mechanism of thyroid hormone action.** *Thyroid* 2002, **12:**441-446.
4. O'Shea PJ, Williams GR: **Insight into the physiological actions of thyroid hormone receptors from genetically modified mice.** *J Endocrinol* 2002, **175:**553-570.
5. Forrest D, Vennstrom B: **Functions of thyroid hormone receptors in mice.** *Thyroid* 2000, **10:**41-52.
6. McKenna NJ, Lanz RB, O'Malley BW: **Nuclear receptor coregulators: cellular and molecular biology.** *Endocrinol Rev* 1999, **20:**321-344.
7. Refetoff S, Weiss RE, Usala SJ: **The syndromes of resistance to thyroid hormone.** *Endocr Rev* 1993, **14:**348-399.
8. Yoh SM, Chatterjee VK, Privalsky ML: **Thyroid hormone resistance syndrome manifests as an aberrant interaction between mutant T3 receptors and transcriptional corepressors.** *Mol Endocrinol* 1997, **11:**470-480.
9. Weiss RE, Refetoff S: **Resistance to thyroid hormone.** *Rev Endocr Metab Disord* 2000, **1:**97-108.
10. Zhang XY, Kaneshige M, Kamiya Y, Kaneshige K, McPhie P, Cheng SY: **Differential expression of thyroid hormone receptor isoforms dictates the dominant negative activity of mutant beta receptor.** *Mol Endocr* 2002, **16:**2077-2092.
11. Kaneshige M, Kaneshige K, Zhu X, Dace A, Garrett L, Carter TA, Kazlauskaite R, Pankratz DG, Wynshaw-Boris A, Refetoff S *et al.*: **Mice with a targeted mutation in the thyroid hormone beta receptor gene exhibit impaired growth and resistance to thyroid hormone.** *Proc Natl Acad Sci USA* 2000, **97:**13209-13214.
12. Parrilla R, Mixson AJ, McPherson JA, McClaskey JH, Weintraub BD: **Characterization of seven novel mutations of the c-*erbA* beta gene in unrelated kindreds with generalized thyroid hormone resistance. Evidence for two "hot spot" regions of the ligand binding domain.** *J Clin Invest* 1991, **88:**2123-2130.
13. Griffith A, Szymko Y, Kaneshige M, Quinonez R, Kaneshige K, Heintz K, Masteroianni M, Kelly M, Cheng SY: **Knock-in mouse model for resistance to thyroid hormone (RTH): an RTH mutation in the thyroid hormone receptor β gene disrupts cochlear morphogenesis.** *J Assoc Res Otolaryngol* 2002, **3:**279-288.
14. Kamiya Y, Zhang XY, Ying H, Kato Y, Willingham MC, Xu J, O'Malley BW, Cheng SY: **Modulation by steroid receptor coactivator-1 of target-tissue responsiveness in resistance to thyroid hormone.** *Endocrinology* 2003, **144:**4144-4153.
15. Pritchard CC, Hsu L, Delrow J, Nelson PS: **Project normal: defining normal variance in mouse gene expression.** *Proc Natl Acad Sci USA* 2001, **98:**13266-13271.
16. Robbins J: **Thyroid hormone transport proteins and the physiology of hormone binding.** In *The Thyroid* 8th edition. Edited by: Braverman LE, Utiger RD. Philadelphia, PA: Lippincott William and Wilkins; 2000:105-120.
17. Sotiriou C, Powles TJ, Dowsett M, Jazaeri AA, Feldman AL, Assersohn L, Gadisetti C, Libutti SK, Liu ET: **Gene expression profiles derived from fine needle aspiration correlate with response to systemic chemotherapy in breast cancer.** *Breast Cancer Res* 2002, **4:**R3.
18. Sadow PM, Chassande O, Gauthier K, Samarut J, Xu J, O'Malley BW, Weiss RE: **Specificity of thyroid hormone receptor subtype and steroid receptor coactivator-1 on thyroid hormone**

action. *Am J Physiol Endocrinol Metab* 2003, **284:**E36-E46.
19. Miller L, Park K, Guo Q, Alkharouf N, Malek R, Lee N, Liu E, Cheng SY: **Silencing of Wnt signaling and activation of multiple metabolic pathways in response to thyroid hormone-stimulated cell proliferation.** *Mol Cell Biol* 2001, **21:**6626-6639.
20. Dillmann WH, Gloss BR: **The role of thyroid hormone receptors in the heart.** *Methods Mol Biol* 2002, **202:**55-70.
21. Fadel BM, Ellahham S, Ringel MD, Lindsay J Jr, Wartofsky L, Burman KD: **Hyperthyroid heart disease.** *Clin Cardiol* 2000, **23:**402-408.
22. Refetoff S, Weiss RE, Usala SJ: **The syndromes of resistance to thyroid hormone.** *Endocr Rev* 1993, **14:**348-399.
23. Kahaly GJ, Matthews CH, Mohr-Kahaly S, Richards CA, Chatterjee VK: **Cardiac involvement in thyroid hormone resistance.** *J Clin Endocrinol Metab* 2002, **87:**204-212.
24. **Gene Ontology Consortium** [http://www.geneontology.org]
25. Reyne Y, Nougues J, Cambon B, Viguerie-Bascands N, Casteilla L: **Expression of c-erbA alpha, c-erbA beta and Rev-erbA alpha mRNA during the conversion of brown adipose tissue into white adipose tissue.** *Mol Cell Endocrinol* 1996, **116:**59-65.
26. Viguerie N, Millet L, Avizou S, Vidal H, Larrouy D, Langin D: **Regulation of human adipocyte gene expression by thyroid hormone.** *J Clin Endocrinol Metab* 2002, **87:**630-634.
27. Pucci E, Chiovato L, Pinchera A: **Thyroid and lipid metabolism.** *Int J Obes Relat Metab Disord* 2000:S109-S112.
28. Huber O: **Structure and function of desmosomal proteins and their role in development and disease.** *Cell Mol Life Sci* 2003, **60:**1872-1890.
29. Koibuchi N, Chin WW: **Thyroid hormone action and brain development.** *Trends Endocrinol Metab* 2000, **11:**123-128.
30. Poguet AL, Legrand C, Feng X, Yen PM, Meltzer P, Samarut J, Flamant F: **Microarray analysis of knockout mice identifies cyclin D2 as a possible mediator for the action of thyroid hormone during the postnatal development of the cerebellum.** *Dev Biol* 2003, **254:**188-199.
31. Chanoine JP, Braverman LE: **The role of transthyretin in the transport of thyroid hormone to cerebrospinal fluid and brain.** *Acta Med Austriaca* 1992, **19 Suppl 1:**25-28.
32. Vincent J, Legrand C, Rabie A, Legrand J: **Effects of thyroid hormone on synaptogenesis in the molecular layer of the developing rat cerebellum.** *J Physiol (Paris)* 1982, **78:**729-738.
33. Madeira MD, Paula-Barbosa MM: **Reorganization of mossy fiber synapses in male and female hypothyroid rats: a stereological study.** *J Comp Neurol* 1993, **337:**334-352.
34. Hall AC, Lucas FR, Salinas PC: **Axonal remodeling and synaptic differentiation in the cerebellum is regulated by WNT-7a signaling.** *Cell* 2000, **100:**525-535.
35. Salinas PC: **Wnt factors in axonal remodelling and synaptogenesis.** *Biochem Soc Symp* 1999, **65:**101-109.
36. Feng X, Jiang Y, Meltzer P, Yen PM: **Thyroid hormone regulation of hepatic genes *in vivo* detected by complementary DNA microarray.** *Mol Endocrinol* 2000, **14:**947-955.
37. Wood WM, Sarapura VD, Dowding JM, Woodmansee WW, Haakinson DJ, Gordon DF, Ridgway EC: **Early gene expression changes preceding thyroid hormone-induced involution of a thyrotrope tumor.** *Endocrinology* 2002, **143:**347-359.
38. Davis PJ, Tillmann HC, Davis FB, Wehling M: **Comparison of the mechanisms of nongenomic actions of thyroid hormone and steroid hormones.** *J Endocrinol Invest* 2002, **25:**377-388.
39. Shupnik MA, Chin WW, Habener JF, Ridgway EC: **Transcriptional regulation of the thyrotropin subunit genes by thyroid hormone.** *J Biol Chem* 1985, **260:**2900-2903.
40. Goodridge AG: **Regulation of the gene for fatty acid synthase.** *Fed Proc* 1986, **45:**2399-2405.
41. Gharbi-Chihi J, Facchinetti T, Berge-Lefranc JL, Bonne J, Torresani J: **Triiodothyronine control of ATP-citrate lyase and malic enzyme during differentiation of a murine preadipocyte cell line.** *Horm Metab Res* 1991, **23:**423-427.
42. Sugisaki T, Noguchi T, Beamer WG, Kozak LP: **Genetic hypothyroid mice: normal cerebellar morphology but altered glycerol-3-phosphate dehydrogenase in Bergmann glia.** *J Neurosci* 1991, **11:**2614-2621.
43. Xiong S, Chirala SS, Hsu MH, Wakil SJ: **Identification of thyroid hormone response elements in the human fatty acid synthase promoter.** *Proc Natl Acad Sci USA* 1998, **95:**12260-12265.
44. Weitzel JM, Kutz S, Radtke C, Grott S, Seitz HJ: **Hormonal regulation of multiple promoters of the rat mitochondrial glycerol-3-phosphate dehydrogenase gene: identification of a complex hormone-response element in the ubiquitous promoter B.** *Eur J Biochem* 2001, **268:**4095-4103.
45. Liu YY, Schultz JJ, Brent GA: **A thyroid hormone receptor alpha gene mutation (P398H) is associated with visceral adiposity and impaired catecholamine-stimulated lipolysis in mice.** *J Biol Chem* 2003, **278:**38913-38920.
46. Barrera-Hernandez G, Park KS, Dace A, Zhan Q, Cheng SY: **Thyroid hormone-induced cell proliferation in GC cells is mediated by changes in G1 cyclin/cyclin-dependent kinase levels and activity.** *Endocrinology* 1999, **140:**5267-5274.
47. Pibiri M, Ledda-Columbano GM, Cossu C, Simbula G, Menegazzi M, Shinozuka H, Columbano A: **Cyclin D1 is an early target in hepatocyte proliferation induced by thyroid hormone (T3).** *FASEB J* 2001, **15:**1006-1013.
48. Gonzalez-Sancho JM, Figueroa A, Lopez-Barahona M, Lopez E, Beug H, Munoz A: **Inhibition of proliferation and expression of T1 and cyclin D1 genes by thyroid hormone in mammary epithelial cells.** *Mol Carcinog* 2002, **34:**25-34. (Erratum in: *Mol Carcinog* 2002, **34:**164)
49. Perez-Juste G, Aranda A: **The cyclin-dependent kinase inhibitor p27(Kip1) is involved in thyroid hormone-mediated neuronal differentiation.** *J Biol Chem* 1999, **274:**5026-5031.
50. Nishikawa A, Kaiho M, Yoshizato K: **Cell death in the anuran tadpole tail: thyroid hormone induces keratinization and tail-specific growth inhibition of epidermal cells.** *Dev Biol* 1989, **131:**337-344.
51. James RA, Sarapura VD, Bruns C, Raulf F, Dowding JM, Gordon DF, Wood WM, Ridgway EC: **Thyroid hormone-induced expression of specific somatostatin receptor subtypes correlates with involution of the TtT-97 murine thyrotrope tumor.** *Endocrinology* 1997, **138:**719-724.
52. Dinda S, Sanchez A, Moudgil V: **Estrogen-like effects of thyroid hormone on the regulation of tumor suppressor proteins, p53 and retinoblastoma, in breast cancer cells.** *Oncogene* 2002, **21:**761-768.
53. Kastan MB, Zhan Q, el-Deiry WS, Carrier F, Jacks T, Walsh WV, Plunkett BS, Vogelstein B, Fornace AJ Jr: **A mammalian cell cycle checkpoint pathway utilizing p53 and GADD45 is defective in ataxia-telangiectasia.** *Cell* 1992, **71:**587-597.
54. el-Deiry WS, Tokino T, Velculescu VE, Levy DB, Parsons R, Trent JM, Lin D, Mercer WE, Kinzler KW, Vogelstein B: **WAF1, a potential mediator of p53 tumor suppression.** *Cell* 1993, **75:**817-825.
55. Jaiswal AS, Narayan S: **p53-dependent transcriptional regulation of the APC promoter in colon cancer cells treated with DNA alkylating agents.** *J Biol Chem* 2001, **276:**18193-18199.
56. Foster MP, Montecino-Rodriguez E, Dorshkind K: **Proliferation of bone marrow pro-B cells is dependent on stimulation by the pituitary/thyroid axis.** *J Immunol* 1999, **163:**5883-5890.
57. Watanabe K, Iwatani Y, Hidaka Y, Watanabe M, Amino N: **Long-term effects of thyroid hormone on lymphocyte subsets in spleens and thymuses of mice.** *Endocr J* 1995, **42:**661-668.
58. Ruan H, Zarnowski MJ, Cushman SW, Lodish HF: **Standard isolation of primary adipose cells from mouse epididymal fat pads induces inflammatory mediators and down-regulates adipocyte genes.** *J Biol Chem* 2003, **278:**47585-47593.
59. Gloss B, Trost S, Bluhm W, Swanson E, Clark R, Winkfein R, Janzen K, Giles W, Chassande O, Samarut J, Dillmann W: **Cardiac ion channel expression and contractile function in mice with deletion of thyroid hormone receptor alpha or beta.** *Endocrinology* 2001, **142:**544-550.
60. Gloss B, Sayen MR, Trost SU, Bluhm WF, Meyer M, Swanson EA, Usala SJ, Dillmann WH: **Altered cardiac phenotype in transgenic mice carrying the delta337 threonine thyroid hormone receptor beta mutant derived from the S family.** *Endocrinology* 1999, **140:**897-902.
61. Taegtmeyer H, Cohen DM: **Overestimating glycolysis in rat heart.** *Am J Physiol Endocrinol Metab* 2002, **283:**E1102-1103. (Author reply E1103-1104)
62. Swanson EA, Gloss B, Belke DD, Kaneshige M, Cheng SY, Dillmann WH: **Cardiac expression and function of thyroid hormone receptor beta and its PV mutant.** *Endocrinology* 2003, **144:**4820-4825.
63. Eisen MB, Brown PO: **DNA arrays for analysis of gene expression.** *Methods Enzymol* 1999, **303:**179-205.
64. Wang E, Miller LD, Ohnmacht GA, Liu ET, Marincola FM: **High-fidelity mRNA amplification for gene profiling.** *Nat Biotechnol* 2000, **18:**457-459.
65. **National Cancer Institute: Center for Cancer Research** [http://nciarray.nci.nih.gov]

66. **Genome Institute of Singapore: supplementary information**
[http://www.gis.a-star.edu.sg/homepage/toolssup.jsp]